Biol. Cell (2010) **102**, 525–537 (Printed in Great Britain) doi:10.1042/BC20100033

multimedia online data Research article

Bimolecular fluorescence complementation analysis of eukaryotic fusion products

Ho-Pi Lin*, Claudius Vincenz†, Kevin W. Eliceiri‡, Tom K. Kerppola† and Brenda M. Ogle*‡§[1]

*Department of Biomedical Engineering, University of Wisconsin-Madison, Madison, WI 53706, U.S.A., †Howard Hughes Medical Institute and Department of Biological Chemistry, University of Michigan-Ann Arbor, Ann Arbor, MI 48109, U.S.A., ‡Laboratory for Optical and Computational Instrumentation, University of Wisconsin-Madison, WI 53706, U.S.A., and §The Material Science Program, University of Wisconsin-Madison, Madison, WI 53706, U.S.A.

Background information. Cell fusion is known to underlie key developmental processes in humans and is postulated to contribute to tissue maintenance and even carcinogenesis. The mechanistic details of cell fusion, especially between different cell types, have been difficult to characterize because of the dynamic nature of the process and inadequate means to track fusion products over time. Here we introduce an inducible system for detecting and tracking live cell fusion products *in vitro* and potentially *in vivo*. This system is based on BiFC (bimolecular fluorescence complementation) analysis. In this approach, two proteins that can interact with each other are joined to fragments of a fluorescent protein and are expressed in separate cells. The interaction of said proteins after cell fusion produces a fluorescent signal, enabling the identification and tracking of fusion products over time.

Results. Long-term tracking of fused p53-deficient cells revealed that hybrid cells were capable of proliferation. In some cases, proliferation was preceded by nuclear fusion and division was asymmetric (69% $\pm$ 2% of proliferating hybrids), suggesting chromosomal instability. In addition, asymmetric division following proliferation could give rise to progeny indistinguishable from unfused counterparts.

Conclusions. These results support the possibility that the chromosomal instability characteristic of tumour cells may be incurred as a consequence of cell fusion and suggest that the role of cell fusion in carcinogenesis may have been masked to this point for lack of an inducible method to track cell fusion. In sum, the BiFC-based approach described here allows for comprehensive studies of the mechanism and biological impact of cell fusion in nature.

Introduction

Fusion between cells of the same type has been observed and extensively studied in a variety of tissues including muscle, bone, liver and placenta (Chen and Olson, 2005; Ogle et al., 2005). In these tissues, fusion products are believed to possess enhanced functions compared with their unfused progenitors. For example, when the trophoblast cells of the placenta fuse to form the syncytiotrophoblast, the syncytiotrophoblast is better able to transport nutrients and hormones across the maternal–fetal barrier than unfused trophoblasts (Hoshina et al., 1982; Benirschke, 1995). Failure of syncytiotrophoblast formation is linked to complications of pregnancy, such as pre-eclampsia (Johansen et al., 1999; Redman and Sargent, 2000). Fusion between cells of different types has also been demonstrated and, in some cases, results in reprogramming of cellular gene expression. For example, fusion of human fibroblasts and murine muscle cells gave rise to fusion products in which human muscle genes are expressed from the fibroblast genome (Blau et al., 1983). The modification of cell fate by fusion was believed by some to be

[1]To whom correspondence should be addressed (email ogle@wisc.edu).
Key words: cell fusion, bimolecular fluorescence complementation (BiFC), live cell imaging, stem cell, cancer.
Abbreviations used: Bach2, BTB and CNC homology 1, basic leucine zipper transcription factor 2; BiFC, bimolecular fluorescence complementation; CBX2, chromobox protein homologue 2; CFP, cyan fluorescent protein; EST, expressed sequence tag; PEG, poly(ethylene glycol); YFP, yellow fluorescent protein.

limited to cultured cells. However, stem cell transplantation for therapeutic purposes led to the discovery that stem cells or their progeny can fuse with a variety of somatic cells *in vivo* and that fusion affects stem cell differentiation (Alvarez-Dolado et al., 2003; Vassilopoulos et al., 2003; Wang et al., 2003; Camargo et al., 2004; Nygren et al., 2004; Ogle et al., 2004; Shi et al., 2004; Ishikawa et al., 2006; Johansson et al., 2008). Intriguingly, some observations suggest that cell fusion is rate-limiting in the progression of some cancers (Parris, 2005; Duelli and Lazebnik, 2007). Thus cell fusion could be important for development, tissue repair and pathogenesis.

Given the potential significance of cell fusion, it is surprising that basic aspects of cell fusion are still largely unknown. A hindrance to progress in this area is the lack of appropriate technology to accurately identify fusion products and to track them over time. Insufficient technology has prevented investigation of the prevalence of cell fusion or its functions. Thus technical advances in this area can contribute to a better understanding of the fundamental characteristics of cell fusion. Such improved approaches could lead to identification of the signals that trigger fusion, the cell surface proteins that mediate fusion and the mechanism(s) that reprogramme and determine the functions of hybrid cells.

Two primary methods are currently employed to detect and track the fusion between living cells. Firstly, cell fusion can be detected using fluorescent dyes. Once inside living cells, these dyes react with intracellular components (i.e. thiol groups, amine groups) to produce cells that are fluorescent. Different dyes are used to label each fusion partner and fusion products are detected based on emissions from both fluorophores. This method is appropriate for short-term *in vitro* studies; however, *in vivo* studies are difficult and the fluorescence signal is lost over time. In addition, other processes can result in membrane transfer between cells, potentially leading to misidentification of fusion events. Fusion events can also be identified by labelling prospective fusion partners using fluorescent proteins [i.e. CFP (cyan fluorescent protein) or YFP (yellow fluorescent protein)]. This method allows long-term tracking of fusion products. However, it can be difficult to distinguish fusion products from cells whose fluorescence signals overlap in densely packed cells in culture or in tissue. In addition, it may be possible for the signal to be transferred to cells via uptake of cellular debris in the absence of fusion. Secondly, cell fusion can be detected by the complementary actions of proteins: most commonly, the lacZ system (Mohler and Blau, 1996) and the *Cre–LoxP* system (Alvarez-Dolado et al., 2003; Ogle et al., 2005). With lacZ gene complementation, the gene is dissected into two fragments and each fragment is introduced into each fusion partner. Enzymatic activity is produced on convergent expression of the two distinct mutant lacZ peptides within single cells or on fusion of cells expressing such mutants. Unfortunately, detection of lacZ complementation requires addition of a substrate and, hence, is not favourable for long-term tractability. With Cre–*LoxP* gene complementation, one fusion partner constitutively expresses Cre recombinase and the other fusion partner harbours a reporter gene placed adjacent to a stop codon flanked by *LoxP* sequences. When exposed to the Cre protein via cell fusion the *LoxP* and stop signals are excised and the reporter gene is expressed. This inducible method enables detection of only true fusion events *in vitro* and *in vivo*. However, generation of the signal requires time for excision of the stop codon and subsequent transcription and translation of the reporter. This delay limits the ability to study events immediately after cell fusion. Thus, although some progress has been made to monitor cell fusion in living cells, there is a paucity of effective means to detect and track fusion products quickly and reliably *in vitro* and *in vivo*.

Here we introduce a new approach to detect and track cell fusion of living cells. The approach is based on BiFC (bimolecular fluorescence complementation), a method originally designed to study protein–protein interactions in living cells (Hu et al., 2002). BiFC is based on the observation that fragments of a fluorescent protein can be genetically dissected into two non-fluorescent fragments. Each fragment is joined to two separate proteins and interaction between these two proteins facilitates the maturation of fluorescent protein assembled from the fluorescent fragments. The location and intensity of BiFC signals have been used to study interactions among a variety of proteins including nuclear, ubiquitin family, membrane, enzymatic and signalling proteins (Kerppola, 2006). Here we use the unique properties of BiFC analysis to detect and track cell fusion events. In brief, any pair of chosen proteins known to interact with each other can be linked to

Figure 1 | Representation of BiFC analysis adapted to detect cell fusion

Two cell populations (A and B) are modified to express non–fluorescent fragments of fluorescent proteins (YFP) joined to proteins that can interact with each other. If a cell of population A fuses with a cell of population B, the two proteins can interact with each other and produce a fluorescent signal.

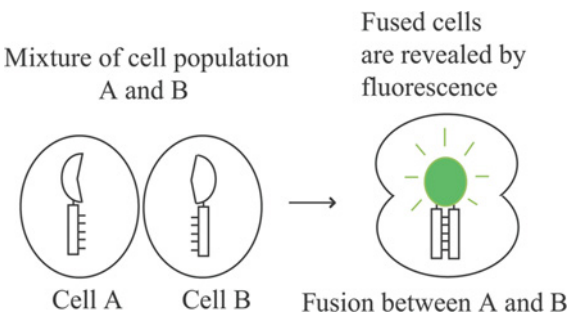

complementary, non-fluorescent fragments and expressed in separate cell populations (Figure 1). In the event of cell fusion, cellular components mix, allowing the two non-fluorescent counterparts to interact and form a fluorescent signal. Due to the absolute requirement for both fragments to form a fluorescent complex, the incidence of false-positives is virtually non-existent and fluorescent signals can be readily detected via either fluorescence microscopy or flow cytometry. Since the coding regions of the two fusion proteins are also brought into the same cell on fusion, the fluorescence intensity increases over time, allowing long-term, live-cell studies. Finally, the availability of databases of established protein–protein interactions (such as http://mint.bio.uniroma2.it) allows great flexibility in coupling protein interactions of interest with fusion events.

Results

An inducible signal for cell fusion using BiFC analysis

To test whether BiFC could be used to detect cell fusion, we tested whether fluorescent protein fragments expressed in different cells could form BiFC complexes after cell fusion. To this end, COS-1 cells were seeded on to two wells that were separately transfected with plasmids encoding VN-Histone H3.1 (VN-H3.1) and YC-Histone H3.1 (YC-H3.1) respectively. VN-H3.1 refers to a plasmid encoding residues 1–172 of the Venus fluorescent protein joined to Histone H3.1, and YC-H3.1 refers to another plasmid encoding the complementary residues 173–238 of YFP joined to Histone H3.1. A nuclear BiFC signal was desirable for initial experiments, since the presence of two or more nuclei at early time points after initiation of fusion supports the likelihood that the signal detected is indeed indicative of cell fusion. Histone H3.1 was selected since two molecules of Histone H3 are known to participate in the formation of a Histone tetramer with Histone H4. This tetramer can subsequently form an octamer with Histones H2A and H2B and is eventually incorporated stably into chromatin and so detected in the nucleus (Verreault, 2000). After transfection, equal numbers of cells in the two wells were co-cultured with cells expressing the complementary YFP fusion protein. PEG [poly(ethylene glycol)] was applied to the co-cultured cells to induce fusion, and the fluorescence of cells cultured in the presence and absence of PEG was compared. As a control, equal numbers of cells (and the same total number of cells as above) that expressed only VN-H3.1 or YC-H3.1 were cultured in the presence of PEG. Cells with detectable fluorescence were counted 1, 3, 6, 9 and 24 h after PEG application using fluorescence microscopy (Figure 2d). Cells containing multiple fluorescent nuclei were observed in the co-cultures that expressed both VN-H3.1 and YC-H3.1 treated with PEG (Figures 2a–2c). These presumably reflect the fusion of multiple cells, including at least one cell from each population. As expected, the fluorescence was typically nuclear (Figures 2a–2c) and fluorescent cells were distributed throughout the culture dishes (Figures 2d and 2e). Control cells that were co-cultured in the absence of PEG produced less than 1% of the number of fluorescent cells observed in cultures treated with PEG to induce cell fusion. These control cells contained two or more nuclei, presumably reflecting spontaneous fusion among COS-1 cells. No fluorescence was detected in control cells that expressed only VN-H3.1 or YC-H3.1 treated with PEG. These results demonstrate that BiFC complexes were produced on co-culture of cells that expressed complementary fluorescent protein fragments by a process that was dramatically enhanced by PEG treatment, consistent with specific detection of cell fusion by BiFC analysis.

To determine how soon BiFC signals could be detected after PEG-induced fusion and to establish the

Figure 2 | Validation of the BiFC approach to detect cell fusion

Two populations of COS-1 cells were transfected overnight with VN-Histone H3.1 and YC-Histone H3.1 respectively. The two populations of cells were then plated together one day prior to induction of fusion by PEG1500. (**a**–**e**) Typical BiFC fusion signals. Fusion signals (BiFC, green) were detected by fluorescence microscopy and images were obtained at high (**a**) and low magnification (**d**). Histone H3.1 was localized to the nucleus (**b**, Hoechst 33142 stain, blue; **c**, **e**, a merge with phase contrast). (**f**) Kinetic analysis of BiFC fusion signals. Two populations of COS-1 cells were transfected with plasmids encoding BiFC partners in the presence or absence of PEG1500. In addition, two populations of COS-1 cells were transfected with the same BiFC complex (i.e. VN-Histone H3.1 + VN-Histone H3.1 or YC-Histone H3.1 + YC-Histone H3.1). The number and location of cells per well with fusion signals were counted over a period of 24 h after fusion was induced. Three wells were counted for each condition. The mixture containing both BiFC partners induced to fuse via PEG showed the most dramatic increase in number of signals over time. In contrast, cell populations containing only one BiFC partner (i.e. VN- or YC-Histone H3.1) showed no formation of BiFC signals. (**g**) Time-lapse imaging of BiFC fusion signals. Cells were prepared as above and images were acquired after PEG-induced fusion at a frequency of 1/10 min over a period of 12 h. The upper panels show fusion signals and the lower panels show the same signals merged with a corresponding phase image. Scale bars in (**a**–**g**), 20 μm.

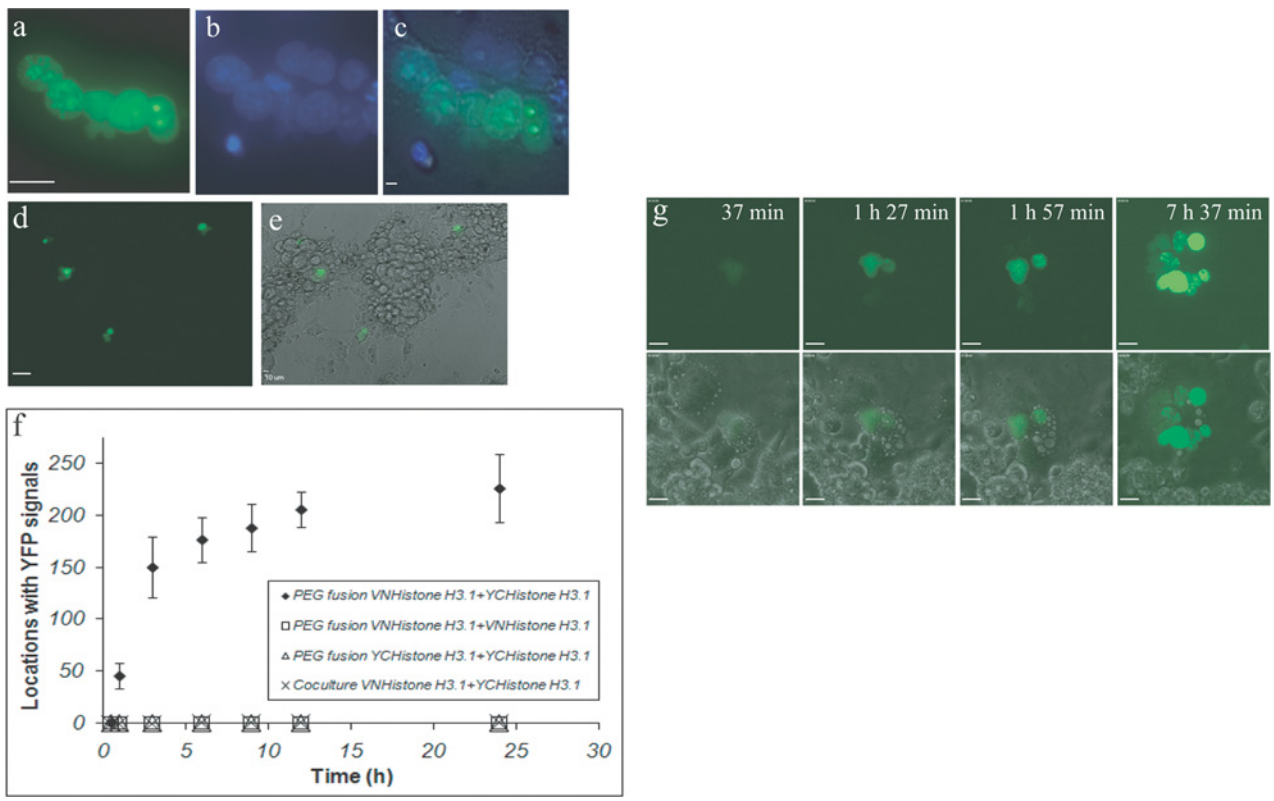

ability of this approach to track products of cell fusion over time, we imaged BiFC complex formation immediately after application of PEG using time-lapse microscopy imaging. Fluorescence was typically detected within 30 min after PEG treatment and increased in intensity over time. This increase was observed in spite of photo-bleaching caused by sequential imaging. A representative result is shown in Figure 2(g) (see also Supplementary Movie S1 at http://www.biolcell.org/boc/102/boc1020525add.htm). The delay in the detection of cell fusion likely reflects the time required for the two non-fluorescent fragments to produce the mature fluorophore (Kerppola, 2006). However, signal formation might also require *de novo* protein synthesis after fusion. To test this possibility, the pattern of signal expression in fusion products was monitored over time in the presence of a protein synthesis blocker, cycloheximide.

Figure 3 | BiFC partners synthesized prior to cell fusion are able to form fusion signals

Two populations of COS-1 cells were transfected with plasmids encoding either VN-CBX2 or YC-Histone H3.1, one day prior to mixing. In addition, a plasmid encoding CFP–Histone H2A (red) was co-transfected with VN-CBX2. At 90 min prior to PEG-induced fusion, co-cultured cells were treated with cycloheximide, a chemical blocker of protein synthesis. Time-lapse imaging was used to track fusion products after application of PEG. Shown is one cell with two nuclei, i.e. the product of one fusion event. Fusion signals (formed by pre-existing BiFC partners) were found in one nucleus first (arrow, from 2 h 30 min to 5 h 50 min after application of PEG). On removal of cycloheximide, new signals (generated as a consequence of newly synthesized BiFC proteins) formed within both nuclei including the partner nucleus (arrowhead). Times shown in white indicate the time period after application of PEG1500, and times shown in black indicate the time period after removing cycloheximide. (**a**) BiFC signals; (**b**) CFP signals corresponding to nuclei of fusion partner containing VN-CBX2; (**c**) YFP/CFP merge; (**d**) phase contrast at close to 150 min after application of PEG; (**e**) quantitative analysis of BiFC fluorescence intensity over time. Zero time in the scatter plot corresponds to the first image in (**a**) (2 h 30 min after PEG treatment); the 210 min in the scatter plot corresponds to removal of cycloheximide. Exposure time was shortened after removal of cycloheximide to prevent overexposure. Scale bars, 10 μm.

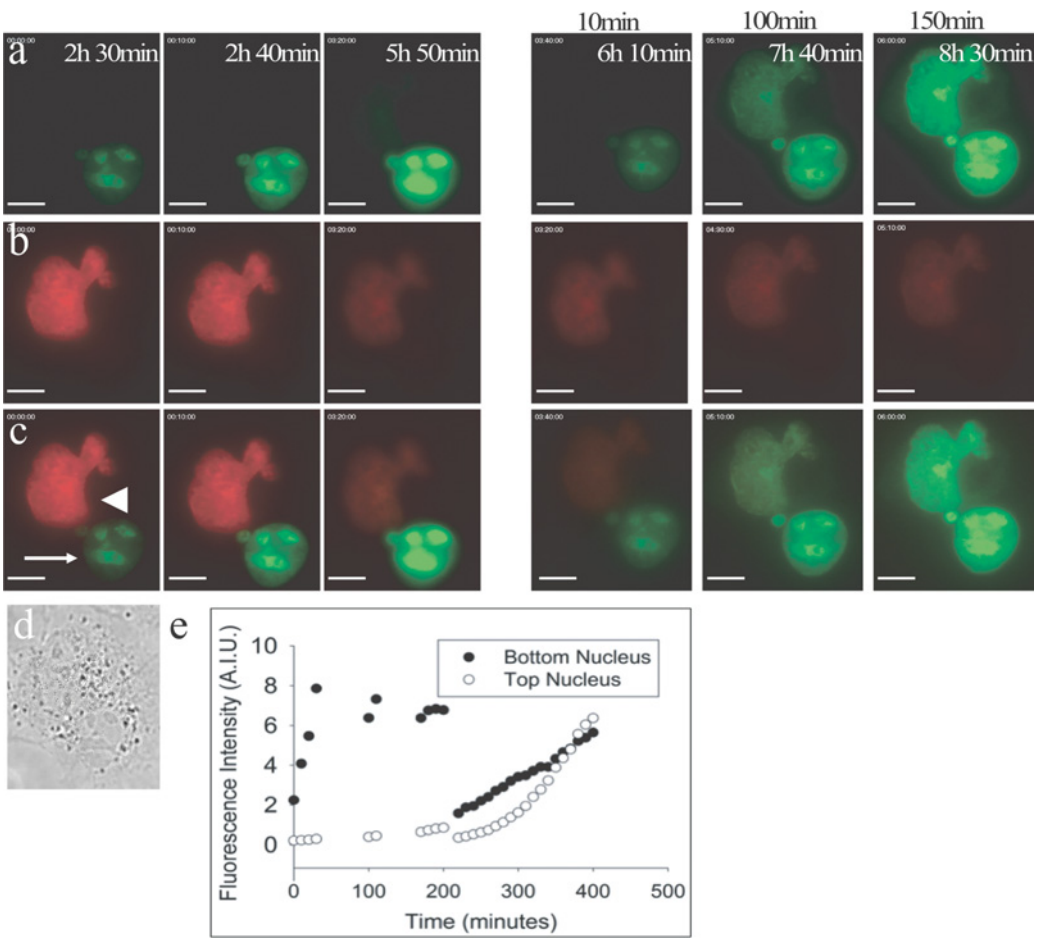

COS-1 cells separately expressing VN-CBX2 (chromobox protein homologue 2), a protein known to interact with Histone H3.1 and YC-Histone H3.1 were co-cultured (Vincenz and Kerppola, 2008). Co-cultures were treated with cycloheximide for 90 min prior to and after PEG-induced fusion. One fusion event with two participating nuclei is shown in Figure 3. A small amount of CFP–Histone H2A (red, Figures 3b and 3c) was co-expressed in COS-1 cells carrying VN-CBX2 so that nuclei of this

Figure 4 | Comparison of the BiFC analysis of cell fusion with alternative methods to detect hybrid cells

Two populations of COS-1 cells were transfected with CFP–c1 (red – whole cell) and YFP–CBX5 (green – nucleus) respectively. The two populations were co-cultured overnight and then exposed to PEG to induce fusion. Putative fusion products should contain both CFP and YFP signals. Such double-positive cells were identified and tracked over time using fluorescence microscopy. (**a**) Tracking of a CFP^+/YFP^+ fusion event. A white arrow denotes a typical putative fusion product containing both red and green signals. Over time, a multinucleate entity forms, confirming a fusion event. (**b**, **c**) Tracking of a false-positive CFP^+/YFP^+ fusion event. A white arrow denotes a typical putative fusion product containing both red and green signals. However, over time the red and green signals separate, indicating that the signals were overlapping and not fused. The last panel of each series shows a merge of CFP/YFP fluorescence with phase contrast. Scale bars in (**a**–**c**), 20 μm.

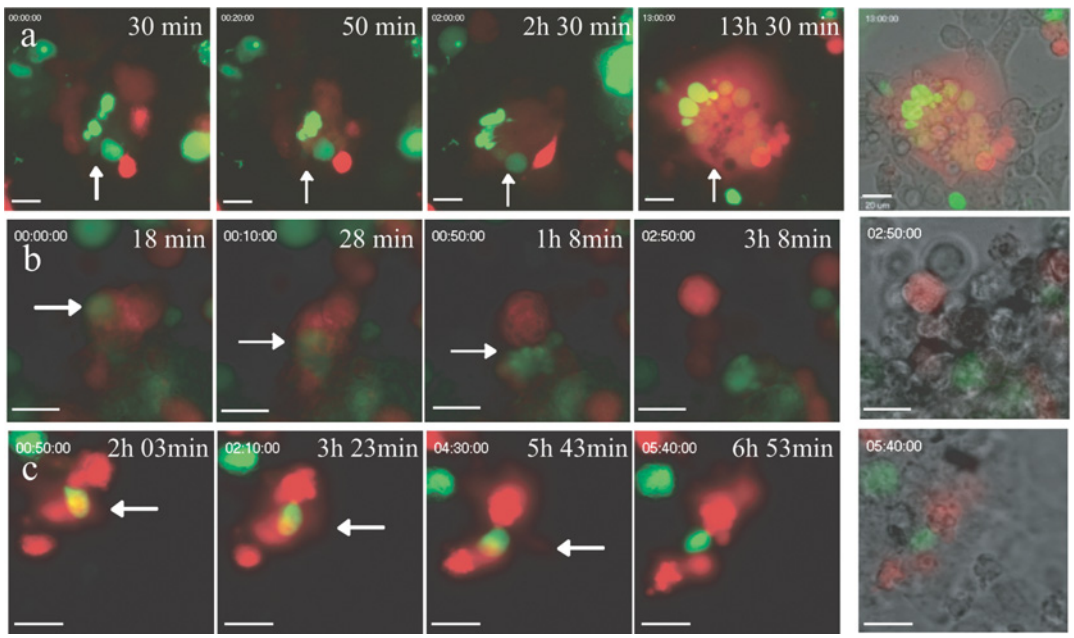

population could be discerned in the absence of or with a delayed BiFC signal. BiFC signals were first formed within one nucleus (arrow) even in the presence of cycloheximide, confirming that BiFC proteins existing prior to the induction of cell fusion can participate in and are sufficient to generate a BiFC signal (Figure 3a). After removal of the cycloheximide, BiFC complexes formed also in the nucleus that encoded VN-CBX2 (arrow and arrowhead). The fact that BiFC complexes formed unequally within the two nuclei while protein synthesis was blocked suggests that the transfer of YC-H3.1 and VN-CBX2 between the two nuclei occurs at unequal rates. This could be attributed at least in part to the distinct mobilities of Histone H3.1 and CBX2 fusions (Ren et al., 2008). Thus proteins produced by cells prior to cell fusion can produce BiFC complexes, obviating the need for fusion protein synthesis in the hybrid cell for detection of cell fusion.

Comparison with existing methods to monitor cell fusion in living cells

Cell fusion can be monitored using cytoplasmic dyes or by expressing reporter genes (i.e. green fluorescent protein, YFP and CFP) in fusion partners and tracking double-labelled cells (i.e. fusion products) over time. To test the specificity and sensitivity of this label approach compared with the BiFC, two populations of COS-1 cells were transfected separately with CFP (whole cell localization) or YFP–CBX5 (nuclear localization). After PEG-induced fusion, optical fields containing double-labelled cells (i.e. putative fusion events) were chosen and these fields were tracked over time using fluorescence time-lapse microscopy. Multiple 'putative' fusion events were identified (i.e. one nuclear YFP signal surrounded by CFP signal), many of which were bona fide fusion events (i.e. YFP signal surrounded by CFP signal persisting over time; Figure 4a). However, false-positive

Figure 5 | Detection of cell fusion via cytosolic BiFC partners

Plasmids YN-Bach2 and YC-Bach2 were transfected into separate populations of COS-1 cells. CFP–Histone H2A (red) was co-transfected with YN-Bach2. After induction of fusion, time-lapse imaging was performed. Fusion signals (green) were mainly found in cytosol and a late joining nucleus was seen, at 12 h 10 min, entering from the lower left corner (arrows).

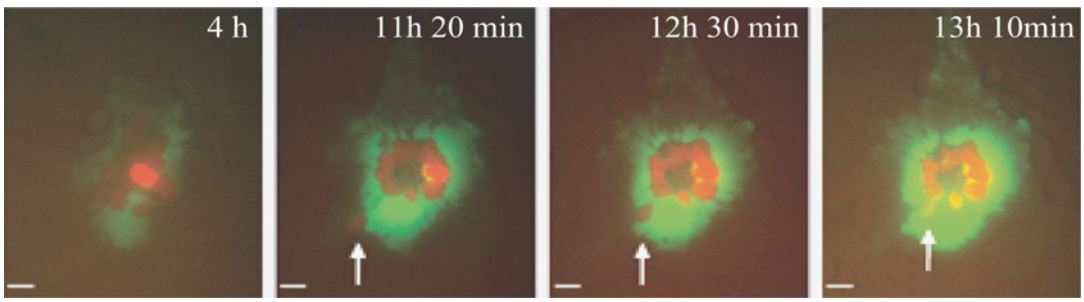

signals exhibiting behaviour shown in Figures 4(b) and 4(c), wherein the two signals eventually separate, were also frequently found (56% ± 8%; see also Supplementary Movies S2–S4 at http://www.biolcell.org/boc/102/boc1020525add.htm). False-positive signals were significantly reduced when putative fusion was defined as two or more nuclear YFP signals coinciding with CFP signals and coupled with bright-field detection and so identification of cell borders (3% ± 1%). Similarly, when fluorescent probes were used to label different populations, the incidence of false-positive cell fusion events using flow cytometry was reported to be as high as 1.53% (Huerta et al., 2002). The percentage of false-positive events is relatively high if one considers that spontaneous fusion events may account for ⩽1% of the total number of cells co-cultured. The limited specificity of this approach will also prove troublesome when studying cell types prone to aggregate (i.e. embryonic stem cells). For these reasons, an inducible signal is desired for detecting fusion products so that true signals do not need to be discriminated from background signal.

Inducible systems that employ the *Cre–LoxP* system have been used to study cell fusion (Alvarez-Dolado et al., 2003; Mohler and Blau, 1996). With this system, a plasmid with stop codon flanked by two *LoxP* sites is placed proximal to a reporter gene (i.e. luciferase). Fusion of a cell harbouring this plasmid with a cell expressing Cre recombinase results in the expression of the reporter gene. In an attempt to compare this inducible system with the BiFC approach to detect cell fusion, COS-1 cells were transfected with a plasmid p231 pCMVe-betaAc-STOP-luc (containing a floxed stop cassette in front of a luciferase gene). Surprisingly, COS-1 cells with transfected plasmid alone (i.e. stop codon in place) showed high levels of luciferase activity. The same plasmid was used to transfect PAECs (porcine aortic endothelial cells) and showed no detectable activity for luciferase. The plasmid has been shown to have functional luciferase activity only after the action of Cre recombinase in other cell types. These results suggest the *Cre–LoxP* approach might not be suitable for some cancer cell lines, which apparently exhibit Cre-like activity or spontaneous suppression of transcription termination.

The other disadvantage of the *Cre–LoxP* system is the delay in detection of the fusion event. The Cre–*LoxP* system requires time for excision of the stop codon and proper protein formation. The generation of BiFC signals also requires some time to form the fluorescence complex, but can be generated with pre-existing proteins.

Detection of cell fusion via cytosolic BiFC partners

BiFC proteins can be selected to alter signal location and signal pattern. As one example, the Bach2 (BTB and CNC homology 1, basic leucine zipper transcription factor 2) was employed as a BiFC protein due to its ability to form homodimers (Oyake et al., 1996) and its cytosolic distribution (Yoshida et al., 2007). When YN-Bach2 and YC-Bach2 were transfected in separate populations of COS-1 cells, inducible signals were collected using time-lapse microscopy after

Figure 6 | Characterization of chimaeric cells by tracking live fusion products for extended periods

Plasmids YN-CBX5 and YC-CBX5 were transfected into separate populations of COS-1 cells. Fusion signals localized mostly within nuclei except while hybrids were in the mitotic stage of the cell cycle. The fate of fusion hybrids in terms of proliferation or death were monitored via time-lapse imaging for 72 h (fusion-BiFC, $n = 220$). To compare the fate of fused hybrids and their unfused counterparts, the same plasmids were sequentially transfected into a single population of COS-1 cells and signals generated were monitored for 72 h (transfection of unfused COS-1, $n = 260$). To compare with alternate fusion detection regimes, YFP and CFP were expressed in separate populations of COS-1 cells and cells with overlapping YFP/CFP signals were monitored for 72 h (fusion-two colour, $n = 152$). (**a**) Fate of fusion products. The fraction of fusion products (or unfused COS-1

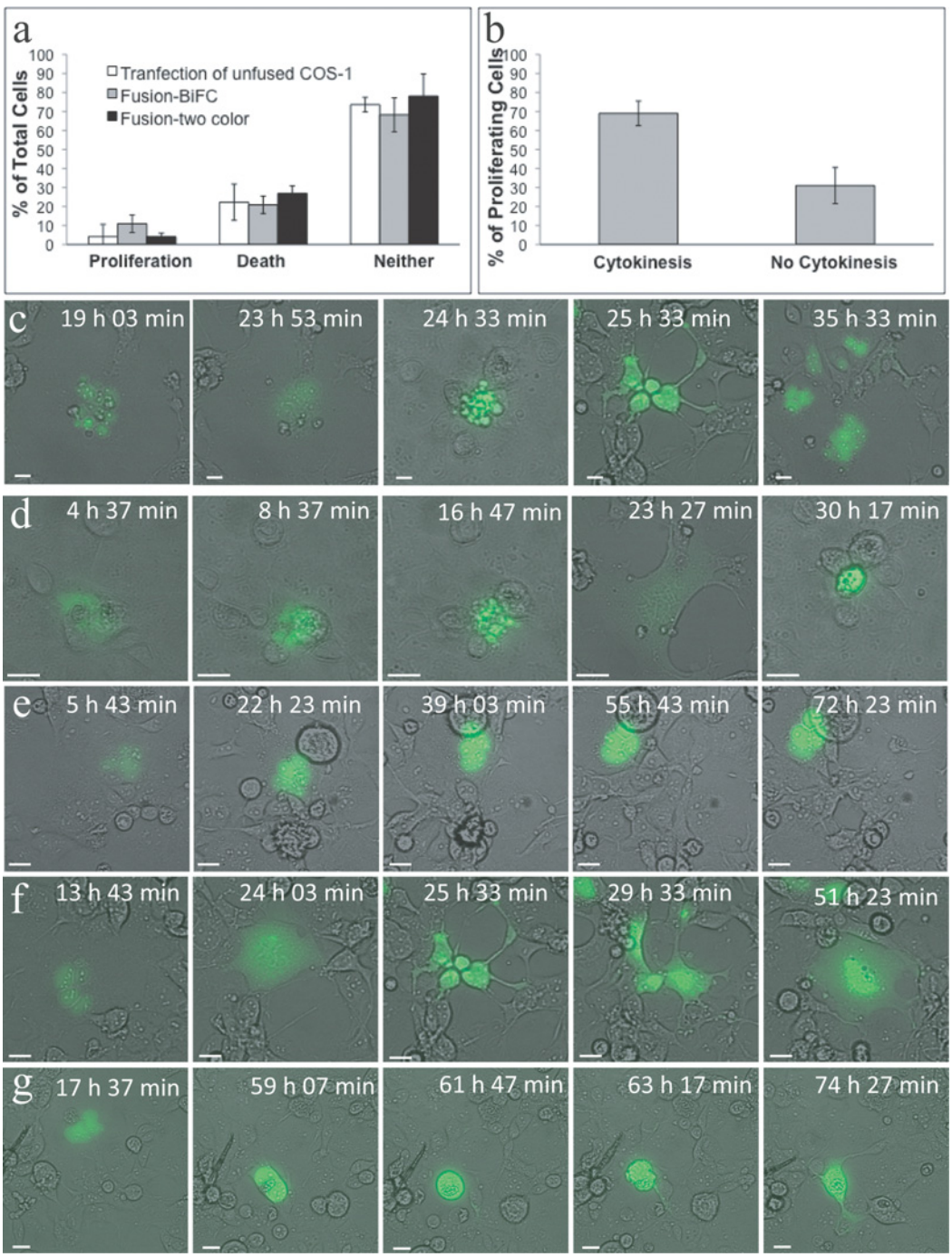

Figure 6 | (contd)

cells) undergoing proliferation, death or neither was determined over the 72 h period. (**b**) Fate of proliferating fusion products. Fusion products detected by BiFC that demonstrated the ability to proliferate ($n = 26$) were further delineated by their ability or inability to undergo complete cytokinesis. (**c**–**g**) Representative time-lapse profile for conditions described in (**a**, **b**). (**c**) Proliferating fusion-BiFC hybrid. (**d**) Fusion-BiFC hybrid undergoing cell death. (**e**) Stable and viable fusion-BiFC hybrid. (**f**) Fusion-BiFC hybrid undergoing DNA replication without completion of cytokinesis to form a multinucleate entity. (**g**) Fusion-BiFC hybrid undergoing DNA replication without apparent cytokinesis to form a cell with a single, giant nucleus. Scale bars in (**a**–**g**), 20 μm; error bars represent S.D.

application of PEG. A small amount of plasmid encoding CFP–Histone H2A (red nuclei, Figure 5) was co-transfected with YN-Bach2 to allow tracking of nuclei prior to cell fusion. BiFC signals were detected in the cytosol (green, Figure 5) and allowed clear visualization of the hybrid border. Typical aggregation of nuclei at the centre of the fused cell was observed, but in this case a view of the cytosol was possible in addition to nuclei. Of note, at least two nuclei appeared to join the fusion event during the imaging cycle (see also Supplementary Movie S5 at http://www.biolcell.org/boc/102/boc1020525add.htm) – perhaps the first documented case of the events leading to spontaneous fusion or alternatively the migration of nuclei within a hybrid (arrows in Figure 5).

Analysis of the characteristics of hybrid cells detected using BiFC analysis

To investigate the characteristics of chimaeric cells, we tracked products of cell fusion containing two or multiple nuclei detected by BiFC analysis over time. We examined the proliferation of hybrid cells, rate of cell death and the overall stability of hybrid cells. We used BiFC subunits linked to the CBX5 chromatin-binding protein as this protein forms homodimers and is enriched within heterochromatic regions, but is displaced from chromatin during mitosis (Cowieson et al., 2000; Hirota et al., 2005). Using transfection conditions identical with those used above, plasmids encoding YN-CBX5 and YC-CBX5 were transfected into separate populations of COS-1 cells and inducible signals were tracked using time-lapse microscopy after application of PEG. Fusion products (containing 2–30 nuclei) were categorized according to cell behaviour over a 72 h time span. Of note, cells were seeded at a high density to promote cell–cell contact and subsequent fusion events. At this seeding density, the growth rate is low and the death rate is high (see Supplementary Figure S1 at http://www.biolcell.org/boc/102/boc1020525add.htm). Most of the hybrid cells detected using BiFC analysis remained stable and viable over the time of observation (72 h), but did not divide ($68\% \pm 9\%$, Figures 6a and 6e; see Supplementary Movie S6 at http://www.biolcell.org/boc/102/boc1020525add.htm). In hybrid cells, cell death was observed ($21\% \pm 5\%$, Figures 6a and 6d; see Supplementary Movie S7 at http://www.biolcell.org/boc/102/boc1020525add.htm), and in other hybrid cells, proliferation of nuclei was observed ($11\% \pm 5\%$, Figures 6a, 6c, 6f and 6g; see Supplementary Movies S8–S10 at http://www.biolcell.org/boc/102/boc1020525add.htm). The frequencies of proliferation and death were not statistically different from unfused counterparts (COS-1 cells sequentially transfected with identical BiFC pairs, Figure 6a), indicating that cell fusion does not inhibit survival of COS-1 cells under the conditions used here. This result was further confirmed as COS-1 fusion products detected using the two-colour method exhibited statistically similar proliferation, death and survival (without proliferation) rates compared with unfused counterparts (Figure 6a).

Of the proliferating hybrids, some completed cytokinesis ($69\% \pm 2\%$) to produce 2, 3, 4 or more daughter cells. Within this population, all progeny inherited uneven nuclear volumes or number. The other population of hybrids failed to complete cytokinesis ($31\% \pm 2\%$), and formed either a multinucleate entity or a cell with one giant nucleus. Hybrids that contained multiple nuclei after proliferation appeared to arise from a regression of the cleavage furrow during cytokinesis (Shi and King, 2005). Hybrids that formed a giant nucleus showed no apparent attempt to undergo cytokinesis. These observations indicate that cell fusion can result in hybrid cells with many different properties, potentially depending on the characteristics of the parental

cells or their environments. Further studies of the effects of cell fusion on the characteristics of hybrid cells and their biological roles will undoubtedly be facilitated by BiFC analysis of cell fusion.

Discussion

We report here what we believe to be a substantial step toward discerning the biological impact of cell fusion. Because the product of a cell fusion event can appear unchanged from an unfused counterpart, a highly specific approach for detection of cell fusion is necessary. The BiFC-based method described here is inducible and highly specific, ensuring that all signals generated represent actual fusion events. The BiFC-based method generates a single-colour fluorescent signal that grows more intense over time and can be tracked using a standard fluorescence imaging system. Further, the BiFC approach allows rapid detection of signals since proteins synthesized prior to fusion can generate a signal. Rapid signal generation is crucial for the study of early fusion events. In contrast, other inducible, single-colour methods, including the Cre–*LoxP* system, require time to excise the *LoxP*-containing cassette, initiate transcription, translation and proper folding of the reporter gene. In addition, the specificity of the Cre–LoxP approach can be compromised if the stop codon can be bypassed in the absence of Cre or cell fusion. In sum, the BiFC-based approach offers the first rapid, specific and relatively simple means to detect cell fusion for long-term studies.

The benefits of this approach are already apparent. Several decades ago, it was demonstrated that fusion of tumour cells with lymphocytes yields metastatic cells (Mekler, 1971) and that cell fusion contributes the phenotypic and genotypic diversity of tumours (Warner, 1975). However, the mechanistic details of these processes have been difficult to study and hence remain largely unknown. Here we monitored fusion among COS-1 cells, a line transformed by deficient SV40 (simian virus 40) virus via perturbation of tumour suppressors, p53 and Rb (retinoblastoma) through large T antigen (Gluzman, 1981). We show that fusion did not inhibit the ability of hybrids to proliferate, although not all proliferating hybrids underwent division ($31\% \pm 2\%$ of proliferating hybrids). Of those hybrids that did undergo cytokinesis after proliferation ($69\% \pm 2\%$ of proliferating hybrids), division was asymmetric with progeny containing unequal numbers of nuclei or volume of nuclei via reductive division (Wang et al., 2003; Duncan et al., 2009) or other mechanisms. Chromosomal rearrangement inherent in these processes lends insight into the mechanism whereby fusion might contribute to the massive chromosomal instability and subsequent genetic diversity of tumour cells. In addition, we observed that some progeny of asymmetric division of hybrids being phenotypically indistinguishable from non-fused counterpart suggests possible underestimation of the significance of fusion. Consistent with both potential outcomes, depolyploidization of tumour cells exposed to radiation can give rise to cells capable of proliferation and uniquely equipped to evade the genotoxic or cytotoxic agent that initially spurred polyploidy (Tao et al., 2008; Ianzini et al., 2009). It is tempting therefore to hypothesize that fusion followed by depolyploidization may enable cancer cells to withstand clinical treatments. This hypothesis and others related to the role of fusion in carcinogenesis will be facilitated by the BiFC approach described here.

The mechanistic details garnering stem cell–somatic cell fusion are also a mystery. It is possible that fusion in this case mimics that of transformed cells, although the process may be entirely different. If it is similar, it is interesting to consider the role of stable, non-proliferative hybrids in stem cell programming or somatic cell reprogramming. Perhaps the quiescent state imposed by fusion (Figure 6e) allows time needed for (re)programming of fused nuclei; of note, nuclear reprogramming could start within one day of fusion (Pereira et al., 2008). A detection method such as BiFC analysis enables robust, long-term detection of fusion and hence could begin to disclose mechanistic details of this elusive process.

It is important to consider the limitations of the BiFC approach so that it can be most effectively and constructively employed. There may, for example, be instances when the two-colour method described above will suffice. The two-colour method provides strength of detection of fusion events in real time. And although this method suffers from a substantial false-positive rate, this problem becomes less significant when fusion events are plentiful. However, when the timing or location of fusion is unclear and the frequency is low (i.e. stem cell/cancer cell–somatic cell fusion), a method such as BiFC analysis could

be the method of choice. One limitation of the BiFC method is that the sensitivity depends on transfection efficiency. The higher the efficiency, the more sensitive the approach is likely to be. In that vein, transient transfection efficiency can only be estimated prior to fusion and so it is difficult to determine or compare the frequency of cell fusion between different fusion partners. However, it would be possible to utilize a bicistronic construct including a reporter to simultaneously measure transfection efficiency. Alternatively, it would be possible to generate stable transformants or utilize viral transduction to circumvent this problem. Another limitation of this approach is the possibility that the formation of the BIFC complex may, under certain circumstances, be irreversible (Tarassov et al., 2008). The possibility that BiFC complexes may form irreversible complexes could limit or enhance the utility of the BiFC assay. In one way, the irreversible nature of the complex could increase long-term stability of the signal and hence enhance the overall sensitivity of the assay. Alternatively, irreversible formation of the BiFC complex might indirectly impact on cell phenotype and function and hence should be carefully tested before long-term tracking experiments. To alleviate this potential drawback, a BiFC pair with high turnover rate might be selected. Finally, it might be possible for a BiFC signal to be generated as a consequence of uptake of cell debris and so generate a false-positive BiFC signal. However, our results indicate that this possibility is rare since a BiFC signal generated from uptake of debris would correspond to a cell with a single nucleus. In all co-cultures described here, BiFC signals detected immediately after mixing fusion always corresponded to cells with two or more nuclei.

The nature of the BiFC system is extremely versatile since selected protein interactions can include any of thousands of documented protein interactions. One can therefore envision not only detecting cell fusion, but also studying protein–protein interactions relevant to the initiation, propagation or (re)programming events associated with cell fusion. In addition, a combination with other variants of fluorescent proteins could be used to perform multicolour BiFC (Hu et al., 2002). In this case, more than two protein interactions or more than two cellular populations could be studied. In such a case, fluorescence signals acquired through different channels could represent unique fusion events or unique consequences of fusion events. Finally, fluorescent fragments could be linked to a membrane protein pair facing either the cytosolic or extracellular side to discriminate fusion events from cell–cell contact and to indicate the location of the fusion pore (Shi et al., 2009). Taken together, the BiFC approach will enable us to gain new insights into a poorly understood cellular process.

Materials and methods

Cell culture

COS-1 cells were maintained in high-glucose DMEM (Dulbecco's modified Eagle's medium) supplemented with 1% L-glutamine, sodium pyruvate, 10% (v/v) FBS (fetal bovine serum) and antibiotics at 37°C in 5% CO_2.

Transfection

COS-1 cells were transfected with different BiFC constructs at 0.5–2 μg per well of a 6-well plate by FuGENE™ 6 (Roche). The ratio of DNA to reagent was kept at 1:3. Cells were kept in a medium containing transfecting material until further preparation for co-culturing the two transfectants. For comparison with unfused COS-1 cells, we sequentially transfected cells with BiFC pairs under identical transfection conditions as those in corresponding experiments.

Live cell imaging

All images were acquired by Nikon TE300, Nikon Diaphot 200 or Olympus IX71 inverted fluorescence microscope with a cooled CCD (charge-coupled-device) camera. YFP fluorescence was measured by excitation at 500 nm and emission at 535 nm. CFP fluorescence was measured by excitation at 436 nm and emission at 470 nm. Fluorescence images were obtained every 10 min for a period of 8–72 h. Prior to image acquisition, fusion hybrids expressing YN- and YC- fusion proteins required incubation at 30°C for 1 h to induce maturation of fluorophore. Cells were maintained in CO_2-independent medium (Gibco) while acquiring images at 30°C (Nikon TE300) or 37°C established by a heated stage (Olympus IX71). Long-term multiposition fluorescence studies were conducted on a Nikon Diaphot 200 equipped with a heated (37°C) chamber, Hamamatsu Orca camera and motorized XY stage (Applied Scientific MS-2000). Cells were imaged in 6-well plates and image acquisition was controlled by μManager software (Vale Lab; University of California-San Francisco).

Generation of BiFC constructs

BiFC constructs were generated as follows: constructs of YC-Histone H3.1, VN-CBX2 were described previously (Vincenz and Kerppola, 2008). CFP–c1 is from Invitrogen. For VN-Histone H3.1, the amino acids 1–172 of Venus were fused to the N-terminus of human Histone H3.1 derived by PCR from an EST (expressed sequence tag). Primers for PCR amplification of Histone H3.1 were as follows: forward primer: 5′- TAGGCTCTAGAGCAGTCTCTGCGCGTACGAAGCAGACTGCTCG-3′; reverse primer: 5′-CACCCGGGATCCTCATCAAGCCCTCTCGCCGCGGATACGACGTGCG-3′. For YFP-, YN-CBX5 or YC-CBX5, full-length YFP, the amino acids 1–172 of YFP (YN) or the amino acids 173–238 of YFP (YC) were fused to the

N-terminus of human CBX5. Primers for PCR amplification of human CBX5 using an EST as the template were as follows: forward primer, 5′-TAGGCTCTAGAGCAGTCTCTATGGGAAAGAAAACCAAGCGGACAG-3′; reverse primer, 5′-TAGGCTCTAGAGCAGTCTCTATGGGAAAGAAAACCAAGCGGACAG-3′. The amino acid sequence shown below denotes the linker bridging fluorescent protein, VN-, YN- or YC- fragments to N-terminal fusion proteins (i.e. Histone H3.1): Asn-Ser-Ser-Ile-Asp-Leu-Ile-Ser-Val-Pro-Val-Asp-Ser-Arg-Ala-Val-Ser. CFP–Histone H2A was constructed using a similar strategy and was provided by Dr Mohamed Aittaleb (Life Sciences Institute, University of Michigan, Ann Arbor, MI, U.S.A.). Plasmids encoding YN- or YC-Bach2 were YFP fragments (amino acids 1–172 or 173–238) fused to the N-terminus of Bach2 (amplified from murine origin) and were provided by Dr Nirmala Rajaram (Department of Biological Chemistry, University of Michigan, Ann Arbor, MI, U.S.A.). Plasmid requests regarding BiFC plasmids and YFP–HP1 should be addressed to Dr Claudius Vincenz or Dr Tom K. Kerppola.

The plasmid p231 pCMVe-betaAc-STOP-luc (containing a floxed stop cassette in front of a luciferase gene) was constructed in Dr Jeffrey Green's laboratory (Laboratory of Cell Biology and Genetics, National Institutes of Health, Bethesda, MD, U.S.A.) and obtained from Addgene (Kaczmarczyk and Green, 2001).

Cell fate determination

Unfused COS-1 cells or PEG-induced hybrids were tracked using the imaging system described above for 72 h. During image analysis, cells exhibiting membrane blebbing and subsequent shrinkage as well as rounded morphology were categorized as cell death. Cells exhibiting sudden relocation of CBX5 and disappearance of nuclear borders followed with or without completion of subsequent cytokinesis were characterized as cell proliferation. Cells lacking signs of either death or proliferation were placed in a third category. A total of 40–70 hybrids were analysed per experiment and three independent experiments were performed. Two micrograms of each plasmid was used either for fusion experiments or for transfecting unfused counterparts. Since 2 μg of plasmids is the maximum amount possible per transfection, sequential transfection of YN-CBX5 or YC-CBX5 was employed in transfecting unfused counterparts.

PEG-induced fusion

Cells were transfected by expression constructs indicated in each experiment overnight. Typically, transfectants expressing each BiFC counterpart were mixed in a 1:1 ratio and co-cultured overnight. After incubation, co-cultured cells were washed once with PBS, and fusion was induced by applying PEG1500 (50%, v/v) directly on culture dishes or slides for 60 s, washed twice with cell culture media and maintained in cell culture media thereafter. Fluorescence signals were monitored by the described inverted fluorescence microscopy system.

Statistical analyses

For comparison of proliferation, death and cellular stability of fusion products and unfused counterparts, a normal distribution was assumed and one-way ANOVA and Student's t test for unpaired samples were used. Data were analysed with JMP 5.0.1 for Windows (SAS Institute, Carey, NC, U.S.A.). A 95% ($P < 0.05$) confidence interval was applied for statistical significance.

Author contribution

Ho-Pi Lin conceived and designed the research, carried out the experimental work, analysed and interpreted the data, and wrote the article. Claudius Vincenz conceived and designed the research, and analysed and interpreted the data. Kevin Eliceiri carried out the experimental work, and analysed and interpreted the data. Tom Kerppola conceived and designed the research, and analysed and interpreted the data. Brenda Ogle conceived and designed the research, analysed and interpreted the data, and wrote the article.

Acknowledgments

We thank Gary Hammersley, Curtis Rueden and Kristen Seashore of the Laboratory for Optical and Computational Instrumentation, and Benjamin Wolter of the UW Cell and Molecular Biology Program, for technical assistance, and Nico Stuurman of the University of California, San Francisco, for help with μManager software.

Funding

This work was supported by the National Institutes of Health [grant numbers AI057358, HL089679]; and the National Institute of General Medical Sciences [grant number R01 GM086213].

References

Alvarez-Dolado, M., Pardal, R., Garcia-Verdugo, J.M., Fike, J.R., Lee, H.O., Pfeffer, K., Lois, C., Morrison, S.J. and Alvarez-Buylla, A. (2003) Fusion of bone-marrow-derived cells with Purkinje neurons, cardiomyocytes and hepatocytes. Nature **425**, 968–973

Benirschke, K.K.P. (1995) Pathology of the Human Placenta, Springer-Verlag, New York

Blau, H.M., Chiu, C.P. and Webster, C. (1983) Cytoplasmic activation of human nuclear genes in stable heterocaryons. Cell **32**, 1171–1180

Camargo, F.D., Finegold, M. and Goodell, M.A. (2004) Hematopoietic myelomonocytic cells are the major source of hepatocyte fusion partners. J. Clin. Invest. **113**, 1266–1270

Chen, E.H. and Olson, E.N. (2005) Unveiling the mechanisms of cell–cell fusion. Science **308**, 369–373

Cowieson, N.P., Partridge, J.F., Allshire, R.C. and McLaughlin, P.J. (2000) Dimerisation of a chromo shadow domain and distinctions from the chromodomain as revealed by structural analysis. Curr. Biol. **10**, 517–525

Duelli, D. and Lazebnik, Y. (2007) Cell-to-cell fusion as a link between viruses and cancer. Nat. Rev. Cancer **7**, 968–976

Duncan, A.W., Hickey, R.D., Paulk, N.K., Culberson, A.J., Olson, S.B., Finegold, M.J. and Grompe, M. (2009) Ploidy reductions in murine fusion-derived hepatocytes. PLoS Genet. **5**, e1000385

Gluzman, Y. (1981) SV40-transformed simian cells support the replication of early SV40 mutants. Cell **23**, 175–182

Hirota, T., Lipp, J.J., Toh, B.H. and Peters, J.M. (2005) Histone H3 serine 10 phosphorylation by Aurora B causes HP1 dissociation from heterochromatin. Nature **438**, 1176–1180

Hoshina, M., Boothby, M. and Boime, I. (1982) Cytological localization of chorionic gonadotropin alpha and placental lactogen mRNAs during development of the human placenta. J. Cell Biol. **93**, 190–198

Hu, C.D., Chinenov, Y. and Kerppola, T.K. (2002) Visualization of interactions among bZIP and Rel family proteins in living cells using bimolecular fluorescence complementation. Mol. Cell **9**, 789–798

Huerta, L., Lamoyi, E., Baez-Saldana, A. and Larralde, C. (2002) Human immunodeficiency virus envelope-dependent cell–cell fusion: a quantitative fluorescence cytometric assay. Cytometry **47**, 100–106

Ianzini, F., Kosmacek, E.A., Nelson, E.S., Napoli, E., Erenpreisa, J., Kalejs, M. and Mackey, M.A. (2009) Activation of meiosis-specific genes is associated with depolyploidization of human tumor cells following radiation-induced mitotic catastrophe. Cancer Res. **69**, 2296–2304

Ishikawa, F., Shimazu, H., Shultz, L.D., Fukata, M., Nakamura, R., Lyons, B., Shimoda, K., Shimoda, S., Kanemaru, T., Nakamura, K., Ito, J., Kaji, Y., Perry, A.C. and Harada, M. (2006) Purified human hematopoietic stem cells contribute to the generation of cardiomyocytes through cell fusion. FASEB J. **20**, 950–952

Johansen, M., Redman, C.W., Wilkins, T. and Sargent, I.L. (1999) Trophoblast deportation in human pregnancy – its relevance for pre-eclampsia. Placenta **20**, 531–539

Johansson, C.B., Youssef, S., Koleckar, K., Holbrook, C., Doyonnas, R., Corbel, S.Y., Steinman, L., Rossi, F.M. and Blau, H.M. (2008) Extensive fusion of haematopoietic cells with Purkinje neurons in response to chronic inflammation. Nat. Cell. Biol. **10**, 575–583

Kaczmarczyk, S.J. and Green, J.E. (2001) A single vector containing modified cre recombinase and LOX recombination sequences for inducible tissue-specific amplification of gene expression. Nucleic Acids Res. **29**, e56

Kerppola, T.K. (2006) Visualization of molecular interactions by fluorescence complementation. Nat. Rev. Mol. Cell Biol. **7**, 449–456

Mekler, L.B. (1971) Hybridization of transformed cells with lymphocytes as one of the probable causes of the progression leading to the development of metastatic malignant cells. Vestn. Akad. Med. Nauk. SSSR **26**, 80–89

Mohler, W.A. and Blau, H.M. (1996) Gene expression and cell fusion analyzed by lacZ complementation in mammalian cells. Proc. Natl. Acad. Sci. U.S.A. **93**, 12423–12427

Nygren, J.M., Jovinge, S., Breitbach, M., Sawen, P., Roll, W., Hescheler, J., Taneera, J., Fleischmann, B.K. and Jacobsen, S.E. (2004) Bone marrow-derived hematopoietic cells generate cardiomyocytes at a low frequency through cell fusion, but not transdifferentiation. Nat. Med. **10**, 494–501

Ogle, B.M., Butters, K.A., Plummer, T.B., Ring, K.R., Knudsen, B.E., Litzow, M.R., Cascalho, M. and Platt, J.L. (2004) Spontaneous fusion of cells between species yields transdifferentiation and retroviral transfer *in vivo*. FASEB J. **18**, 548–550

Ogle, B.M., Cascalho, M. and Platt, J.L. (2005) Biological implications of cell fusion. Nat. Rev. Mol. Cell Biol. **6**, 567–575

Oyake, T., Itoh, K., Motohashi, H., Hayashi, N., Hoshino, H., Nishizawa, M., Yamamoto, M. and Igarashi, K. (1996) Bach proteins belong to a novel family of BTB-basic leucine zipper transcription factors that interact with MafK and regulate transcription through the NF-E2 site. Mol. Cell. Biol. **16**, 6083–6095

Parris, G.E. (2005) Clinically significant cancer evolves from transient mutated and/or aneuploid neoplasia by cell fusion to form unstable syncytia that give rise to ecologically viable parasite species. Med. Hypotheses **65**, 846–850

Pereira, W.C., Khushnooma, I., Madkaikar, M. and Ghosh, K. (2008) Reproducible methodology for the isolation of mesenchymal stem cells from human umbilical cord and its potential for cardiomyocyte generation. J. Tissue Eng. Regen. Med. **2**, 394–399

Redman, C.W. and Sargent, I.L. (2000) Placental debris, oxidative stress and pre-eclampsia. Placenta **21**, 597–602

Ren, X., Vincenz, C. and Kerppola, T.K. (2008) Changes in the distributions and dynamics of polycomb repressive complexes during embryonic stem cell differentiation. Mol. Cell. Biol. **28**, 2884–2895

Shi, D., Reinecke, H., Murry, C.E. and Torok-Storb, B. (2004) Myogenic fusion of human bone marrow stromal cells, but not hematopoietic cells. Blood **104**, 290–294

Shi, Q. and King, R.W. (2005) Chromosome nondisjunction yields tetraploid rather than aneuploid cells in human cell lines. Nature **437**, 1038–1042

Shi, Y., Barton, K., De Maria, A., Petrash, J.M., Shiels, A. and Bassnett, S. (2009) The stratified syncytium of the vertebrate lens. J. Cell Sci. **122**, 1607–1615

Tao, Y., Zhang, P., Girdler, F., Frascogna, V., Castedo, M., Bourhis, J., Kroemer, G. and Deutsch, E. (2008) Enhancement of radiation response in p53-deficient cancer cells by the Aurora-B kinase inhibitor AZD1152. Oncogene **27**, 3244–3255

Tarassov, K., Messier, V., Landry, C.R., Radinovic, S., Serna Molina, M.M., Shames, I., Malitskaya, Y., Vogel, J., Bussey, H. and Michnick, S.W. (2008) An *in vivo* map of the yeast protein interactome. Science **320**, 1465–1470

Vassilopoulos, G., Wang, P.R. and Russell, D.W. (2003) Transplanted bone marrow regenerates liver by cell fusion. Nature **422**, 901–904

Verreault, A. (2000) *De novo* nucleosome assembly: new pieces in an old puzzle. Genes Dev. **14**, 1430–1438.

Vincenz, C. and Kerppola, T.K. (2008) Different polycomb group CBX family proteins associate with distinct regions of chromatin using nonhomologous protein sequences. Proc. Natl. Acad. Sci. U S A. **105**, 16572–16577

Wang, X., Willenbring, H., Akkari, Y., Torimaru, Y., Foster, M., Al-Dhalimy, M., Lagasse, E., Finegold, M., Olson, S. and Grompe, M. (2003) Cell fusion is the principal source of bone-marrow-derived hepatocytes. Nature **422**, 897–901

Warner, T.F. (1975) Cell hybridization: an explanation for the phenotypic diversity of certain tumours. Med. Hypotheses **1**, 51–57

Yoshida, K., Obata, S., Ono, M., Esaki, M., Maejima, T. and Sawada, H. (2007) TPA-induced multinucleation of a mesenchymal stem cell-like clone is mediated primarily by karyokinesis without cytokinesis, although cell–cell fusion also occurs. Eur. J. Cell Biol. **86**, 461–471

Received 16 March 2010/18 June 2010; accepted 1 July 2010

Published as Immediate Publication 1 July 2010, doi:10.1042/BC20100033

Biol. Cell (2010) **102**, 525–537 (Printed in Great Britain) doi:10.1042/BC20100033

online data

Supplementary online data

Bimolecular fluorescence complementation analysis of eukaryotic fusion products

Ho-Pi Lin*, Claudius Vincenz†, Kevin W. Eliceiri‡, Tom K. Kerppola† and Brenda M. Ogle*‡§[1]

*Department of Biomedical Engineering, University of Wisconsin-Madison, Madison, WI 53706, U.S.A., †Howard Hughes Medical Institute and Department of Biological Chemistry, University of Michigan-Ann Arbor, Ann Arbor, MI 48109, U.S.A., ‡Laboratory for Optical and Computational Instrumentation, University of Wisconsin-Madison, WI 53706, U.S.A., and §The Material Science Program, University of Wisconsin-Madison, Madison, WI 53706, U.S.A.

Figure S1 | Growth rate of COS-1 cells seeded at high density

COS-1 cells used for fusion experiments were seeded at high-density (~95%) confluency. At this confluency, the cells are in plateau phase and so undergo minimal net growth during the period of time typically monitored for cell fusion (i.e. 1–4 days after seeding). Shown here is a typical growth curve (from three separate experiments) for COS-1 cells at the confluency used for cell fusion experiments, although BiFC transduction and fusion were not induced in this case. Arrow indicates typical time point for induction of fusion (d1) after mixing of BiFC transfected populations (d0).

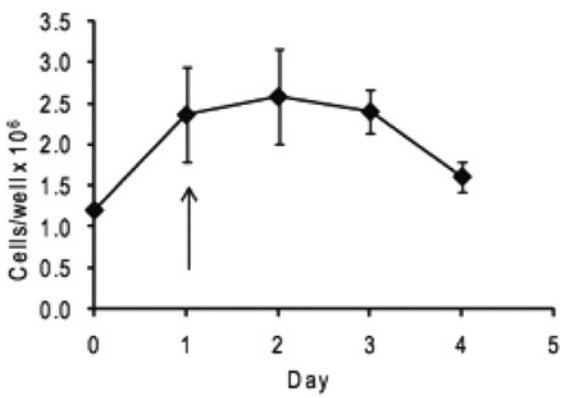

Received 16 March 2010/18 June 2010; accepted 1 July 2010
Published as Immediate Publication 1 July 2010, doi:10.1042/BC20100033

[1]To whom correspondence should be addressed (email ogle@wisc.edu).